ISSN 1063-7826, Semiconductors, 2012, Vol. 46, No. 7, pp. 929–936. © Pleiades Publishing, Ltd., 2012.
Original Russian Text © A.A. Andreev, V.M. Andreev, V.S. Kalinovsky, P.V. Pokrovsky, E.I. Terukov, 2012, published in Fizika i Tekhnika Poluprovodnikov, 2012, Vol. 46, No. 7, pp. 952–959.

SEMICONDUCTOR STRUCTURES, LOW-DIMENSIONAL SYSTEMS, AND QUANTUM PHENOMENA

Evaluation of the Conversion Efficiency of Thin-Film Single-Junction (*a*-Si:H) and Tandem (μ*c*-Si:H + *a*-Si:H) Solar Cells by Analysis of the Experimental Dark and Load Current–Voltage (*I–V*) Characteristics

A. A. Andreev, V. M. Andreev, V. S. Kalinovsky^, P. V. Pokrovsky, and E. I. Terukov

Ioffe Physical–Technical Institute, Russian Academy of Sciences, St. Petersburg, 194021 Russia

^e-mail: vitak.sopt@mail.ioffe.ru

Submitted December 28, 2011; accepted for publication January 11, 2012

Abstract—The aim of the study is to apply a method commonly used to determine the efficiency of multijunction nanoheterostructure III–V solar cells by analysis of the dark current–voltage (*I–V*) characteristics to such an unconventional semiconducting material as amorphous silicon. *a*-Si:H and *a*-Si:H/μ*c*-Si:H *p–i–n* structures without a light-scattering sublayer or an antireflection coating are studied. The results of measurements of the dark *I–V* characteristics demonstrate that the voltage dependence of the current has several exponential portions. The conversion efficiency of solar cells (SCs) is calculated for each portion of the dark *I–V* characteristic. This yields a dependence of the potential SC efficiency on the generation current density or on the photon flux. The observed agreement between the data derived from the experimental characteristics and results of calculations can be considered satisfactory and acceptable, thus the method suggested for measurement and analysis of dark *I–V* characteristics and tested earlier on SCs based on crystalline III–V compounds acquires a universal nature. The analysis of the characteristics of *p–i–n* amorphous silicon structures and the calculation of potential efficiencies, based on this analysis, extend the authors' understanding of this class of devices and make it possible to improve the technology and photoconversion efficiency of SCs of this kind.

DOI: 10.1134/S1063782612070044

1. INTRODUCTION

Despite the large volume of earlier studies of solar cells (SCs) based on amorphous silicon, their dark current–voltage (*I–V*) characteristics have been insufficiently studied. There have been separate publications [1, 2] in which the general form of the *I–V* characteristics of a particular cell and their simplest description were given; however, studies of this kind are not systematic. No attempts have been made, either, to relate specific features of the dark *I–V* characteristics of amorphous semiconductor structures to the efficiency of SC's based on these structures. Three goals are pursued by this study. The first is to measure the forward dark *I–V* characteristics for a set of single-junction cells based on amorphous silicon *a*-SiH and μ*c*-SiH + *a*-Si:H tandems. The second is to analyze the forward dark *I–V* characteristics and to determine the dominant charge-transport mechanisms. The third is to estimate, on the basis of the data obtained, the maximum achievable (potential) photoconversion efficiency of the cells by the following parameters: the pre-exponential factor J_{0i}, the diode coefficient A, and the quality factor of the *p–n* junction, all found from the experimental forward dark *I–V* characteristics. This is to be done by using a calculation procedure based on equations relating the efficiency η and the photogenerated current J_g to the parameters A and J_{0i} of the dark *I–V* characteristics, first suggested for photovoltaic converters based on III–V materials in [3, 4]. The results of these calculations are compared with the efficiencies found by measuring the light *I–V* characteristics of SCs based on amorphous silicon (*a*-Si:H) and an *a*-Si:H + μ*c*-Si:H tandem.

2. SAMPLE FABRICATION

The *p–i–n* amorphous silicon structures were fabricated by the successive deposition of three layers onto glass and quartz substrates with a preliminarily deposited current-conducting contact layer of indium-tin oxide (ITO): boron-doped *p*-type layer, intrinsic *i* layer, and phosphorus-doped *n*-type layer. Further, a contact layer of aluminum was deposited. The silicon layers were deposited in the glow discharge plasma of silane (SiH_4) diluted up to 6% with hydrogen. For doping to yield the *p*- and *n*-types, gases were added to the silane: diborane B_2H_6 and phosphine (PH_3), respectively. The substrate temperature was 300°C. The whole process was monitored in situ by optical interferometry, which made it possible both to determine the layer thicknesses and, to a certain

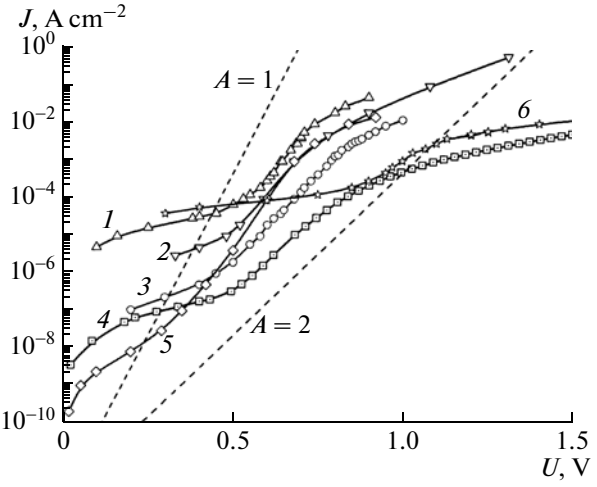

Fig. 1. Experimental forward dark I–V characteristics of an a-Si:H SC (curves *1*–*5*) and a μc-Si:H + a-Si:H tandem SC (curve *6*), measured at room temperature.

extent, monitor their quality by estimating the relative refractive index of the film being deposited. The thickness of the p layer did not exceed 10 nm, and that of the i layer, 450 nm. The fabrication process of amorphous silicon p–i–n structures has been more than once described in ample detail in available publications, and, therefore, we only give its brief description here. The structure based on μc-Si:H primarily differed in the technique used to produce the i layer. In this case, the plasma discharge power was raised by a factor of 2 or more, and silane was diluted with hydrogen in the range from 7–8 at % to the topmost 20 at %. The dilution with hydrogen and the higher plasma discharge power transformed the film growth mode to that of "growth–etching," which favored the formation of silicon nanocrystals 10–30 nm in size, embedded in the amorphous matrix. The microstructure of this material was monitored by high-resolution transmission electron microscopy. Fabrication of the required microstructure was facilitated and controlled by a magnetic field provided by small (0.5 × 0.5 cm) alternating-sign permanent magnets arranged on a plane and situated outside the discharge zone, behind the anode electrode. The microcrystalline silicon μc-Si:H obtained under conditions of strong dilution with hydrogen has an energy gap 0.2–0.3 eV wider than that of a-Si:H [5, 6]. This circumstance opens up prospects for the fabrication of a double structure, a tandem SC formed by two successively formed p–i–n structures based on μc-Si:H on top of a-Si:H and electrically connected by a heavily doped n^{++}–p^{++} tunnel junction serving as an internal ohmic contact. Because the μc layer is composed of a wider-gap material, it is hoped that the spectral sensitivity range of the tandem cell will be wider, with the photovoltage and efficiency, accordingly, becoming higher. However, the whole gain in efficiency may be lost if the ohmic resistance of the connecting n^{++}–p^{++} tunnel contact is high. Losses will be mainly observed in the photocurrent and the fill factor.

We studied the dark and light I–V characteristics of several cells based on a-Si:H and a μc-Si:H + a-Si:H tandem. We emphasize once again that the goal of obtaining cells with maximum efficiency was not pursued. On average, the efficiencies of the a-Si:H cells under study were in the range of 4–6%.

3. EXPERIMENTAL RESULTS

The dark I–V characteristics were measured by a direct-contact method on an installation with automatically recorded results. The external bias was varied from 0 to 3 V, which made it possible to study, if no breakdown occurred, specific features of the I–V characteristics for the third portion of the dark I–V characteristic, or, in other words, in the "superinjection" range, i.e., under conditions of exhausted diffusion transport and current control by other processes. In an exponential approximation of this portion, the diode factor always exceeded 2 ($A > 2$), and approximation of the entire of this portion with series ohmic resistance R_s is not correct in a wide range of external biases. However, in the initial region of the transition from the "recombination-diffusion" process to "superinjection" (up to 1.5 V), it seems quite acceptable. For the main group of a-Si:H p–i–n structures studied, the forward bias was chosen within the range 0–1.5 V.

The "light" (load) I–V characteristics were measured on a sunlight simulator operating in the "constant current mode." The spectrum of a KGM (halogen) incandescent lamp was adjusted with light filters. This system is convenient in operation and enables measurements in selected spectral ranges. However, the photon flux in it is lower than the standard AM1.5 value and a correction coefficient is required. We found this coefficient by comparing data obtained on a simulator with those under exposure to high unscreened Sun in June–July, ~1000 W m^{-2}.

The experimental forward dark I–V characteristics of the samples under study are presented as follows. The a-Si:H samples: no. 187, curve *2* in Fig. 1; no. 191, curve *4* in Fig. 1 and curve *3* in Fig. 2; no. 247 curves *1* in Figs. 1 and 2; no. 2916, curve *3* in Fig. 1; no. 5320, curve *5* in Fig. 1; the tandem structure: no. 250, curves *6* and *5* in Figs. 1 and 2, respectively. For rough estimation, Fig. 1 shows by dashed lines the exponentials calculated with the diode coefficients $A = 2$ and 1. It can be seen that the dark I–V characteristics of all the samples contain, at least, three clearly pronounced segments. Within each separate segment of the I–V characteristic, the experimental dependences are exponentials of the type $J_0\exp(eV/AkT)$, with varying values of the diode coefficient A (diode quality factor). Most of the studied dark I–V characteristics of the a-Si:H SCs contain, at

bias voltages of 0.55 to 0.75 V, a certain "median" portion with a diode coefficient that has a characteristic value of $A = 2-1$, which is indicative of mixed recombination (Sah–Noyce–Shockley) and diffusion (Shockley) [7, 8] charge transport mechanisms in the space-charge region (SCR) of the *p–i–n* junctions studied. Figure 2 shows detailed fitting of two most typical SC samples, *a*-Si:H and a μ*c*-Si:H + *a*-Si:H tandem, to the experimental *I–V* characteristics. It can be seen that, for *a*-Si:H SC no. 191, represented by curve *3*, the recombination-type charge-transport mechanism $A = 2$ is dominant in the "median" portion, whereas for sample no. 247, curve *1*, a gradual transition from the recombination-type charge-transport mechanism to a purely diffusion mechanism with $A = 1$ is observed with increasing forward voltage. The experimental forward dark *I–V* characteristic of the μ*c*-Si:H + *a*-Si:H tandem SC (sample no. 250, curve *6* in Fig. 1 and curve *3* in Fig. 2) has the following specific features: the "median" portion is shifted along the voltage scale to higher voltages, by approximately the amount of the relative change in the open-circuit voltage of the tandem SC (V_{oc}), to 1.4 eV and the diode coefficient is equal to its doubled value for the "recombination" portion of the single-junction *a*-Si:H cell, i.e., $A = 4$ (Fig. 2). In terms of the model suggested in [3, 4], this corresponds to the following: the diode coefficient of the multijunction SC is an arithmetic sum of coefficients ($A = A_1 + A_2 + ... + A_n$) and the pre-exponential factor (J_0) is the geometric mean $J_0 = \sqrt[n]{J_{0_1} J_{0_2} ... J_{0_n}}$ of the pre-exponential factors of all its constituent photoactive junctions. Thus, we have for the "median" portion of the μ*c*-Si:H + *a*-Si:H tandem SC a dominant "recombination" mechanism of charge transport in the SCR from the constituent photoactive *p–i–n* diodes, $A = 4$ and $J_0 = 1.6 \times 10^{-8}$ A cm^{-2}. Using the values $J_{0r} = 1 \times 10^{-8}$–$2 \times 10^{-11}$ A cm^{-2}, obtained by fitting of the experimental dark *I–V* characteristics of the *a*-Si:H SC, we can estimate the pre-exponential factor for μ*c*-Si:H of the photoactive junction in the μ*c*-Si:H + *a*-Si:H tandem SC under study, i.e., $J_{0\mu c} \approx 1 \times 10^{-5}$–$2.5 \times 10^{-7}$ A cm^{-2}.

Comparison of the *I–V* characteristics for the entire set of samples shows that all the curves are qualitatively similar and differ only in particular parameters of their portion segments: A and J_0. The general run of the curves on the whole corresponds to that of a "classical" *I–V* characteristic for a *p–n* junction [9]. The *I–V* characteristics have three clearly pronounced portions. The initial, "tunnel-trap" portion, observed at low voltages of up to 0.3–0.4 V, is described by an exponent of the exponential function $\exp(eV/AkT)$, with the diode coefficient $A > 2$, and a pre-exponential factor J_{0t} in the range 5×10^{-5} to 1.6×10^{-9} A cm^{-2}. The main, "median" portion at voltages of 0.45–0.85 V has A within the range 2.0–1.0, and J_{0r} of 5×10^{-9} to 1.6×10^{-11} A cm^{-2}. The third portion, observed

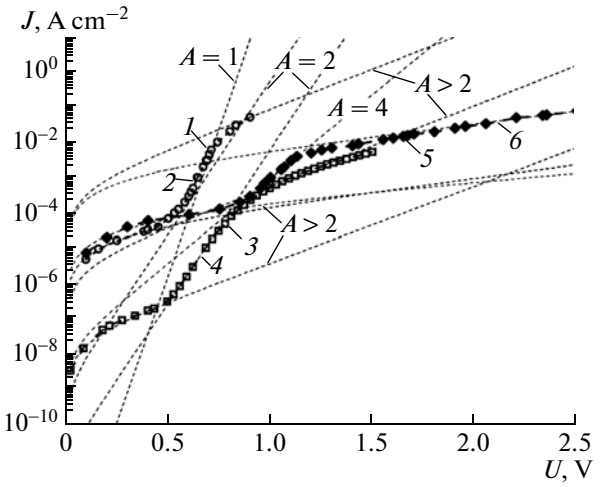

Fig. 2. Experimental forward dark *I–V* characteristics of two *a*-Si:H SCs (sample nos. 191 and 247) and μ*c*-Si:H + *a*-Si:H tandem SC (sample no. 250): curves *1*, *3*, and *5*, experiment, room temperature; curves *2*, *4*, and *6*, calculation (fitting). Curve *1* contains four exponential portions: "tunnel-trap" with $A > 2$, $J_{0(A>2)} = 3.0 \times 10^{-5}$ A cm^{-2}, "recombination" with $A = 2$, $J_{0(A=2)} = 1.2 \times 10^{-9}$ A cm^{-2}; and "diffusion" with $A = 1$, $J_{0(A=1)} = 7.6 \times 10^{-15}$ A cm^{-2}; and "superinjection" with $A > 2$, $J_{0(A>2)} = 4.5 \times 10^{-4}$ A cm^{-2}. Curve *4* contains three exponential portions: "tunnel-trap" with $A > 2$, $J_{0(A>2)} = 2.7 \times 10^{-8}$ A cm^{-2}; "recombination" with $A = 2$, $J_{0(A=2)} = 1.3 \times 10^{-11}$ A cm^{-2} and "superinjection" with $A > 2$, $J_{0(A>2)} = 3.0 \times 10^{-6}$ A cm^{-2}. Curve *5* contains three exponential portions: "tunnel-trap" with $A > 2$, $J_{0(A>2)} = 2.7 \times 10^{-8}$ A cm^{-2}; "recombination" with $A = 4$, $J_{0(A=2)} = 1.3 \times 10^{-11}$ A cm^{-2}; and "superinjection" with $A > 2$, $J_{0(A>2)} = 3.0 \times 10^{-6}$ A cm^{-2}.

at bias voltages exceeding 0.8 V, has $A > 2$, and J_{0i} in the range from 5×10^{-4} to 2.6×10^{-6} A cm^{-2}. In the most general case, the "median" portion is interpreted in accordance with the value of the diode coefficient, $A \approx 2-1$, as resulting from a "recombination" process supplemented with a "diffusion" contribution. For some of the samples (nos. 5320, 187, 247), this portion can be reliably subdivided into two: in the lower range of biases, a clearly pronounced "recombination" component is observed, whereas with increasing bias voltage, there occurs a transition to a purely "diffusion" (Shockley) mechanism with the diode coefficient $A = 1$. The third portion ($U_c > 0.8$ V and $A > 2$) is commonly defined in some reports [10] as the "superinjection" portion, and we will adopt this terminology. The increase in the parameter to $A > 2$ may be due to various mechanisms. These include: current limitation by the space charge of injected electrons and holes, uncompensated in the region of the *p–n* junction [10]; emission-tunneling processes in the contact regions [11]; and, at even higher voltages creating a field strength of $E \approx 10^6$ V cm^{-1}, "tunnel-field hop-

Table 1

Structure	Charge transport mechanism								R_s, (Ω cm^2)
	tunnel-trap			recombination			emission-tunneling		
	J_{0t}, A cm^{-2}	A	U_1, V	J_{0r}, A cm^{-2}	A	U_2, V	J_{0i}, A cm^{-2}	A	Ω/exp
a-Si:H sample no. 191	2.1×10^{-8}	>2	0.45	2×10^{-11}	2	0.83	2.6×10^{-6}	>2	7.5/0.1
a-Si:H sample no. 246	8×10^{-7}	>2	0.5	5.3×10^{-11}	2	0.85	2×10^{-5}	>2	1/0.1
a-Si:H sample no. 2916	4×10^{-7}	>2	0.45	1×10^{-10}	2	0.85	8.6×10^{-5}	>2	5/0.1
a-Si:H + μ-Si:H sample no. 250	9×10^{-5}	>2	0.9	1.6×10^{-8}	4	1.1	3.2×10^{-4}	>2	1/0.01

Table 2

Structure	Charge transport mechanism										R_s, (Ω cm^2)
	tunnel-trap		U_1	recombination		diffusion		U_2	emission-tunneling		
	J_{0t}, A cm^{-2}	A	V	J_{0r}, A cm^{-2}	A	J_{0d}, A cm^{-2}	A	V	J_{0i}, A cm^{-2}	A	Ω/exp
a-Si:H, no. 5320	6×10^{-9}	>2	0.3	9.6×10^{-11}	2	3.6×10^{-15}	1	0.8	2.5×10^{-3}	>2	1/0.1
a-Si:H, no. 187	7×10^{-6}	>2	0.4	4×10^{-10}	2	2.3×10^{-15}	1	0.85	5.6×10^{-6}	>2	1/0.1
a-Si:H, no. 247	3×10^{-5}	>2	0.45	1.2×10^{-9}	2	7.6×10^{-15}	1	0.8	4.5×10^{-4}	>2	3.5/0.1

ping" phenomena of the multistage-tunneling type (Fowler–Nordheim) [8]. Since a solar cell based on amorphous materials operates at voltages of about 1 V, the detailed physical nature of these processes is not of fundamental importance for calculations of the photoelectric conversion efficiency. The third portion of the I–V characteristic is more likely to be important as an indicator that the current rise rate has started to fall. This process is equivalent to an increase in resistance in the current circuit, although the physical process is in fact much more complex. In view of the aforesaid, the complex physical processes can be simply simulated for the initial part of the third portion, at 1–1.5 V, by an equivalent ohmic resistance R_s whose value is found by fitting of the calculated I–V curves to the experimental characteristics (Fig. 2). A brief comment should be added to the above general description of dark I–V characteristics. It is important to emphasize that the "recombination-diffusion" process is observed in all the samples under study. This is indicative of the rather high quality of the material of the cells. For amorphous silicon fabricated by an unoptimized technology and for, e.g., alloys of amorphous silicon with carbon and some other materials, the quality of the p–n junction is, as a rule, deteriorated and the "recombination-diffusion" component of the I–V characteristics may not be observed at all. Charge transport in materials of this kind was considered in [12].

The results of detailed processing of the experimental forward dark I–V characteristics as a sum of the portions corresponding to different charge transport mechanisms in the SCR at various bias voltages are listed in Tables 1 and 2. Table 1 lists the parameters of the structures under study with the dominant recombination mechanism of charge transport in the SCR of the p–i–n junction in the "median" portion of the dark I–V characteristics.

Table 2 summarizes the parameters of the p–i–n structures with mixed charge transport mechanisms in the "median" portion of the I–V characteristics (Figs. 1, 2): of the "recombination" type in the initial part, of the "diffusion" type at high voltages, and of a gradual transition between these two.

The last column in the tables presents, separated by a slash, the series ohmic resistances R_s of SCs, found by fitting to the experimental I–V characteristics (Fig. 1), and those used to calculate the dependences of the efficiency η on the generation current J_g. In the numerator, the initial part of the "superinjection" region is simply simulated with an equivalent ohmic resistance, and in the denominator, with an exponential with $A > 2$. Figure 3 shows the "light" I–V characteristics of the studied SC samples. The efficiencies at the optimal-load point, found by the standard method

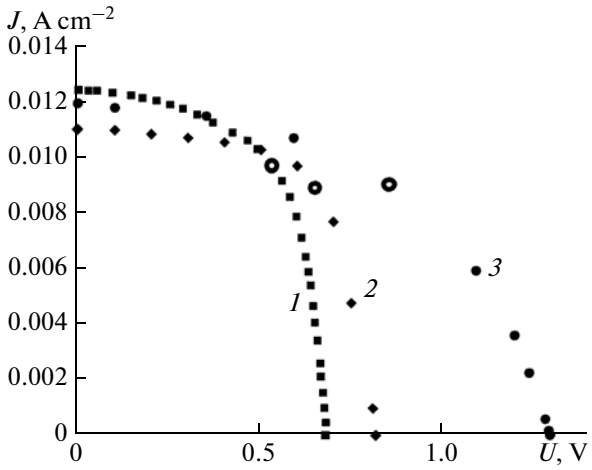

Fig. 3. Experimental light characteristics of *a*-Si:H SCs (curves *1*, *2*) and a μ*c*-Si:H + *a*-Si:H tandem SC (curve *3*), measured at room temperature and AM1.5 solar radiation. The large-diameter circles in the load curve are points corresponding to the optimal load, i.e., to the maximum efficiency, further used in Figs. 4, 5, and 6.

and used in a comparison with the calculated values, are presented in Figs. 4, 5, and 6. It can be seen in these figures that the experimental values of the efficiency (point *5*) lie below the calculated potential efficiencies (curves *3* and *4*). As already noted, this is an expected result because the calculation disregards the loss by light reflection and some other aspects of the post-growth technology.

4. EVALUATION OF THE PHOTOCONVERSION PARAMETERS FROM THE DARK *I–V* CHARACTERISTICS

As shown in reports devoted to III–V-compound-based SCs, the dark *I–V* characteristics can be rather informative for evaluating and prognosticating the parameters of photovoltaic converters of this kind [3, 4]. We introduce into consideration for subsequent analysis a common functional dependence of the forward dark *I–V* characteristics, which includes all the experimentally observed portions of the *I–V* characteristics, identified as segments of a common curve. The complete *I–V* characteristic was obtained by summation of the components corresponding to different portions of the *I–V* characteristic:

$$J = J_{0t}(\exp(V_\varphi/A_t\varepsilon) - 1) + J_{0r}(\exp(V_\varphi/A_r\varepsilon) - 1) + J_{0d}(\exp(V_\varphi/A_d\varepsilon) - 1). \quad (1)$$

where $\varepsilon = kT/q$.

The dark zero-resistance $J–V_\varphi$ characteristic (1) can be approximated by three segments, for each of which the dependence of the voltage in the SCR on the dark current has the form [3]:

$$V_\varphi = A\varepsilon\ln(J/J_0 + 1). \quad (2)$$

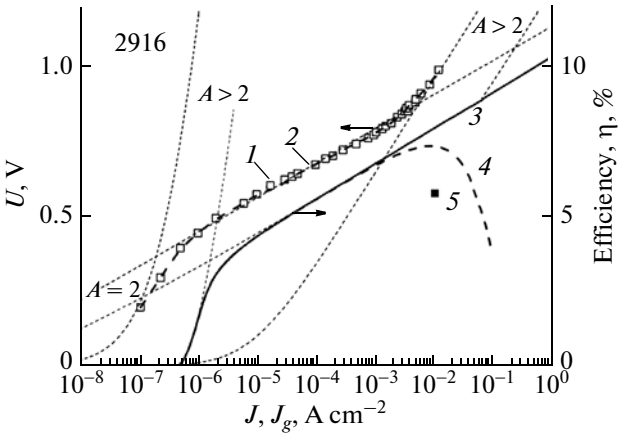

Fig. 4. Experimental and calculated characteristics of an *a*-Si:H SC (sample no. 2916): forward dark *I–V* characteristic (*J–V*): (*1*) experiment and (*2*) calculation; generation current (J_g)–efficiency (η) of the SC: (*3*, *4*) calculation ($R_s = 0$, $R_s \approx 5\ \Omega\ \text{cm}^2$), (*5*) experiment, AM1.5. Portions of the characteristics: $A > 2$, $J_{0(A>2)} = 4.1 \times 10^{-7}$ A cm^{-2}; $A = 2$, $J_{0(A=2)} = 1.15 \times 10^{-10}$ A cm^{-2}; $A > 2$, $J_{0(A>2)} = 8.6 \times 10^{-6}$ A cm^{-2}.

Such a "segment approximation" makes it possible to smooth the calculated functional *I–V* characteristic by mathematical averaging of the values of the *I–V* characteristics in the joining areas of various segments. As demonstrated by the experience of working with such a calculated curve, it is extremely useful in analytical data processing and becomes simply necessary

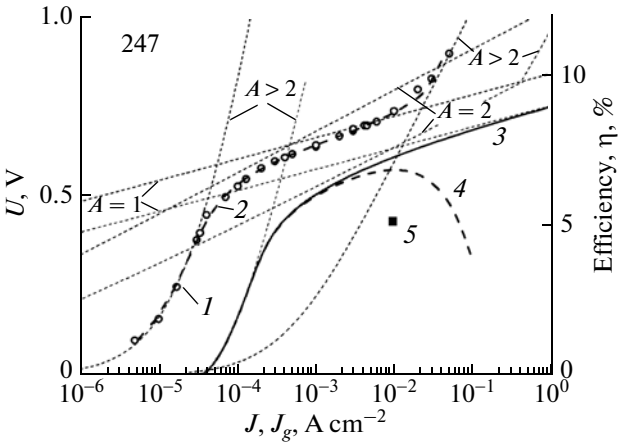

Fig. 5. Experimental and calculated characteristics of an *a*-Si:H SC (sample no. 247): forward dark *I–V* characteristic (*J–V*): (*1*) experiment and (*2*) calculation; generation current (J_g)–efficiency (η) of the SC: (*3*, *4*) calculation ($R_s = 0$, $R_s = 3.5\ \Omega\ \text{cm}^2$), (*5*) experiment, AM1.5. Portions of the characteristics: $A > 2$, $J_{0(A>2)} = 3.0 \times 10^{-5}$ A cm^{-2}; $A = 2$, $J_{0(A=2)} = 1.2 \times 10^{-9}$ A cm^{-2}; $A = 1$, $J_{0(A=1)} = 7.6 \times 10^{-15}$ A cm^{-2}; $A > 2$, $J_{0(A>2)} = 4.5 \times 10^{-4}$ A cm^{-2}.

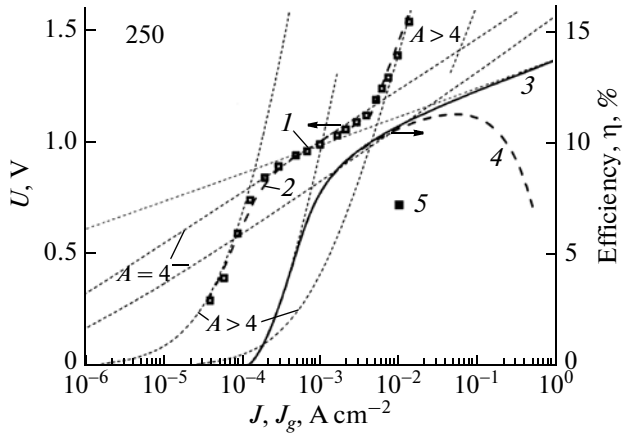

Fig. 6. Experimental and calculated characteristics of a μ*c*-Si:H + *a*-Si:H tandem SC (sample no. 250): forward dark *I–V* characteristic (*J–V*): (*1*) experiment and (*2*) calculation; generation current (J_g)–efficiency (η) of the tandem SC: (*3*, *4*) calculation ($R_s = 0$, $R_s = 1\ \Omega\ \text{cm}^2$), (*5*) experiment, AM1.5. Portions of the characteristics: $A > 4$, $J_{0(A>4)} = 1.0 \times 10^{-4}$ A cm^{-2}; $A = 4$, $J_{0(A=4)} = 1.4 \times 10^{-8}$ A cm^{-2}; $A > 4$, $J_{0(A>4)} = 3.2 \times 10^{-4}$ A cm^{-2}.

when one deals with multijunction structures (tandem, triplet, etc.). In the general case, in the region of joining of the *I–V* characteristic's segments, the "voltage" and "current" boundaries between neighboring segments are given by

$$\begin{cases} V_{n(n+1)} = \dfrac{A_n A_{(n+1)}}{A_n - A_{(n+1)}} \varepsilon \ln(J_{0n}/J_{0(n+1)}) \\ J_{n(n+1)} = \dfrac{J_{0n}^{A_n/(A_n - A_{(n+1)})}}{J_{0(n+1)}^{A_{n+1}/(A_n - A_{(n+1)})}}, \end{cases} \tag{3}$$

where n and $(n + 1)$ are the indices of neighboring segments.

The "light" (load) *I–V* characteristic (for simplicity, we restrict our consideration to a single segment) is obtained from the corresponding segment of the dark *I–V* characteristic and has the form $J = J_g - j$:

$$\begin{cases} V_\varphi = A\varepsilon \ln\left(\dfrac{(J_g - j)}{J_0}\right) \\ j = J_g - J_0 \exp\left(\dfrac{V_\varphi}{A\varepsilon}\right), \end{cases} \tag{4}$$

where $\varepsilon = kT/q$.

For an open circuit mode, $j = 0$ and $V = V_{oc}$. Then, from (4) follows the equation

$$J_g = J_0 \exp\left(\frac{V_{oc}}{A\varepsilon}\right), \tag{5}$$

which has the same pre-exponential factor as the corresponding segment of the dark *I–V* characteristic and coincides in its form with the expression for the dark *I–V* characteristic. The same is true for the continuous function of adjoining segments.

Further, to evaluate the photoconversion parameters, it is necessary to find a correlation between the efficiency of a solar cell and the generation current. A full set of equations describing this correlation was given in [4], and in a more concise form, in [3]. Therefore, it seems inappropriate to present these cumbersome expressions here. We only report the physical meaning of this analysis. The derivative of the power (JV_φ) from Eqs. (4) at the optimal-load point is zero. Solution of the transcendental equation yields the expression:

$$\begin{cases} V_{oc} = V_m + E \ln\left(1 + \dfrac{V_m}{E}\right) \\ \left(1 + \dfrac{V_m}{E}\right) \exp\left(\dfrac{V_m}{E}\right) = \exp\left(\dfrac{E_{oc}}{E}\right), \end{cases} \tag{6}$$

where $E \equiv A\varepsilon$. Using the rearrangements made in [3, 4], we find the maximum power generated by a cell at the optimal-load point:

$$P_m = J_g V_m^2/(V_m + E). \tag{7}$$

Then the efficiency is given by

$$\eta = J_m V_m / P_{inc} = \frac{J_g}{P_{inc}} \frac{V_m^2}{V_m + E} = \frac{V_\eta}{V_{conv}}. \tag{8}$$

Since the ratio of the incident power P_{inc} to the generation current at a fixed solar radiation spectrum, $\dfrac{P_{inc}}{J_g} = V_{conv}$, is independent of the light intensity, the full dependence of the efficiency η on the generation current J_g is also proportional to the concentration ratio of solar radiation and can be expressed in terms of the parameter V_η, defined as the "effective" voltage [3, 4], by

$$V_\eta \equiv \frac{V_m^2}{V_m + E}. \tag{9}$$

Using this formula (9), we can express J_g in terms of V_η and obtain a full expression for the $J_g(\propto C)$–$V_\eta(\propto \eta)$ dependence for the entire set of segments in the *I–V* characteristic of a photovoltaic converter. The effect of the series resistance of the entire structure, R_s (contact resistance and the resistance of the tunnel junction), is accounted for by the introduction of a correcting equation, $V_{\eta o} = V_\eta + R_s$. The calculations are made by a special program using the expressions presented in this communication and data obtained by fitting to the experimental dark *I–V* characteristics of the SCs.

The results of these calculations for *a*-Si:H sample nos. 247 and 2916 and the μ*c*-Si:H + *a*-Si:H tandem (sample no. 250) are presented in Figs. 4, 5, and 6, which combine the following characteristics: dark *J*–*V* and generation current–efficiency (J_g–η). It can be seen from the figures that curves *3* and *4* of the J_g–η characteristics are constituted by the same portion segments as those for the dark *J*–*V* characteristics (curves *1*, *2*). It can be seen that, in the working range of the generation current densities, the role of a factor limiting the potential efficiency of the SC samples under study (curves *3*) is played by the "recombination" charge transport mechanism ($A = 2$ for *a*-Si:H SC and $A = 4$ for the tandem SC). This circumstance accounts for the somewhat higher experimental and calculated efficiency values obtained for sample no. 2916, compared with sample no. 247, because it has a pre-exponential factor J_{0r} that is an order of magnitude smaller and, naturally, a higher open-circuit voltage. For the SCs under study, as the current density J_g or incident light intensity is increased, the efficiency η becomes highly affected by the series resistance R_s of a solar cell (see Figs. 4, 5, and 6; curves *4*) and by the "superinjection" region. However, finding a correlation between the nature of the exponential function in the "superinjection" region and the SC parameters requires a special study.

Thus, our calculation procedure based on parameters obtained by analysis of the experimental dark *I*–*V* characteristics demonstrates the ultimate potential of the growth technique and indicates that opportunities for improving the efficiency of SCs based on amorphous materials are far from being exhausted.

5. CONCLUSIONS

The fundamental role of dark *I*–*V* characteristics in estimation of the photovoltaic conversion efficiency of *a*-Si:H SCs was demonstrated for the first time for *p*–*i*–*n* structures based on amorphous hydrogenated silicon. Analysis of the dark *I*–*V* characteristics enables the effective control over, and improvement of, the technological process for fabrication of *a*-Si:H *p*–*i*–*n* structures. This is particularly important for multijunction solar cells (tandems, triplets), for which the quality of photoactive *p*–*i*–*n* junctions, the balance of currents and resistances of separate elements, and other parameters dependent on post-growth technologies constitute an intricate physical pattern, which is difficult to explain and optimize without an understanding of the dominant charge-transport mechanisms in the SCR of the amorphous *p*–*i*–*n* structures, gained by analysis of the dark *I*–*V* characteristics.

The dark *I*–*V* characteristics of a rather broad group of *a*-Si:H solar cells fabricated at different times with certain differences in the growth parameters were measured. Nevertheless, the solar cells show a similarity in the shapes of their dark *I*–*V* curves and the characteristic portion segments of these curves, and make it possible to distinguish common fundamental aspects of the charge-transport mechanisms.

Of fundamental importance is the presence in all cases of common portions in the dark *I*–*V* characteristics: "tunnel-trap" and "emission-tunnel" segments with a diode quality factor $A > 2$; a "recombination" segment with $A = 2$; and that of the "diffusion" type with $A = 1$. Elements with these mechanisms of charge transport in the *p*–*n* junction have an efficiency of about, or somewhat higher than, 5%. This result is characteristic of cells with the simplest structure, which have no built-in antireflection or light-scattering layers.

Data for the tandem cell, reported in this communication, are rough tentative estimates, but development of a well-elaborated technique for fabrication of tandems and triplets based on μ*c*-Si:H + *a*-Si:H *p*–*i*–*n* structures is a promising way to improve the efficiency of photovoltaic converters based on amorphous materials.

The conversion of unconcentrated solar radiation (AM1.5) by the *a*-Si:H-based solar cells under study is governed by the "recombination" mechanism of charge transport in the SCR of the *p*–*i*–*n* junctions. The method for analysis of the experimental dark *I*–*V* characteristics, previously suggested and tested for multijunction solar cells based on crystalline III–V compounds, is also applicable to *p*–*i*–*n* structures based on amorphous hydrogenated silicon and can be considered universal.

Despite the comparatively low efficiency, amorphous silicon seems to be, owing to its specific properties (ecological safety; low weight of thin films and, accordingly, low consumption of the material; and the possibility for being used on flexible substrates) extremely promising for various fields of photoelectric power engineering. This material is irreplaceable in certain areas of application, and, therefore, its intensive studies are to be continued.

ACKNOWLEDGMENTS

This study was supported in part by the Ministry of Education and Science of the Russian Federation (State contract no. 16.516.11.6053) and the Federal Targeted Program (State contract nos. 16.513.11.3084 and 16.526.12.6017).

REFERENCES

1. A. Mitiga, P. Fiorini, M. Falconieri, and F. Evangelisti, J. Appl. Phys. **66**, 2667 (1989).
2. T. J. McMahon, B. G. Yacobi, and A. Madan, J. Non-Cryst. Solids **66**, 375 (1984).
3. V. S. Kalinovsky and V. M. Andreev, in *Proceedings of the 25th European Photovoltaic Solar Energy Conference*

and 5th World Conference on Photovoltaic Energy Conversion (Valencia, Spain, 2010), p. 979.

4. V. M. Andreev, V. V. Evstropov, V. S. Kalinovskii, V. M. Lantratov, and V. P. Khvostikov, Semiconductors **43**, 644 (2009).
5. A. A. Andreev, A. V. Andrianov, B. Y. Averbouch, R. Mavljanov, S. B. Aldabergeniva, M. Albrecht, and H. P. Strunk, J. Solid State Phenom. **51–52**, 249 (1996).
6. A. Roth, F. J. Comes, and W. Beyer, in *Proceedings of the 11th Energy Conversion Photovoltaic Solar Energy Conference* (Montereux, Swizerland, 1992), p. 594.
7. W. Shockley and H. J. Queisser, J. Appl. Phys. **32**, 510 (1961).
8. S. M. Sze, *Physics of Semiconductors Devices* (Wiley Intersci., New York, 1981; Mir, Moscow, 1984), rus. p. 110.
9. A. Farenburkh and R. Bube, *Fundamentals of Solar Cells: Photovoltaic Solar Energy Conversion* (Academic, New York, 1983; Energoatomizdat, Moscow, 1987).
10. G. Lampert and P. Mark, *Injection Currents in Solids* (Academic, New York, 1970; Mir, Moscow, 1973).
11. B. L. Sharma and R. K. Purohit, *Semiconductor Heterojunctions* (Pergamon, Oxford, 1974; Sov. radio, Moscow, 1979).
12. A. A. Andreev, Semiconductors **42**, 1334 (2008).

Translated by M. Tagirdzhanov